NATIONAL ENERGY TECHNOLOGY LABORATORY

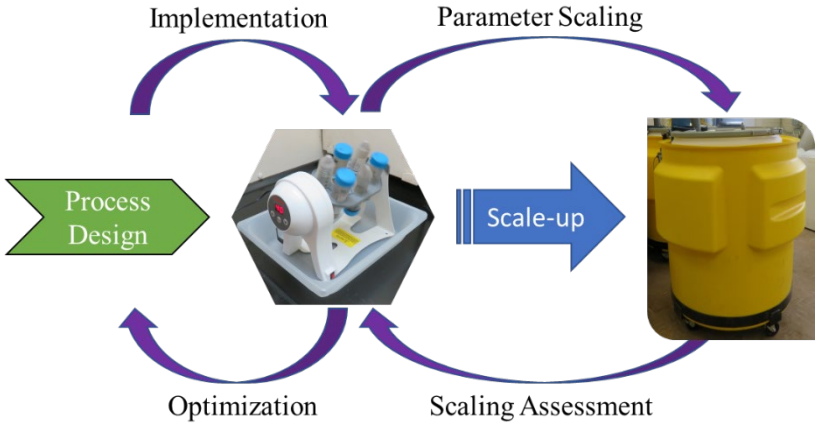

Strategies to Recover Easily-Extractable Rare Earth Elements and Other Critical Metals from Coal Waste Streams and Adjacent Rock Strata Using Citric Acid

26 August 2022

U.S. DEPARTMENT OF ENERGY | NATIONAL ENERGY TECHNOLOGY LABORATORY

Office of Fossil Energy and Carbon Management

DOE/NETL-2022/3732

Disclaimer

Cover Illustration: Process design for implementing bench-scale experiments and scaling up.

Suggested Citation: Yang, J.; Bauer, S.; Verba, C. *Strategies to Recover Easily-Extractable Rare Earth Elements and Other Critical Metals from Coal Waste Streams and Adjacent Rock Strata Using Citric Acid*; DOE.NETL-2022.3732; NETL Technical Report Series; U.S. Department of Energy, National Energy Technology Laboratory: Albany, OR, 2022; p. 28. DOI: 10.2172/1884275

An electronic version of this report can be found at:

https://netl.doe.gov/energy-analysis/search

https://edx.netl.doe.gov/offshore

Strategies to Recover Easily-Extractable Rare Earth Elements and Other Critical Metals from Coal Waste Streams and Adjacent Rock Strata Using Citric Acid

Jon Yang[1,2], Sophia Bauer[1,2], Circe Verba[1]

[1]National Energy Technology Laboratory, 1450 Queen Avenue SW, Albany, OR 97321, USA

[2]NETL Support Contractor, 1450 Queen Avenue SW, Albany, OR 97321, USA

DOE/NETL-2022/3732

26 August 2022

NETL Contacts:

Circe A. Verba, Principal Investigator

R. Burt Thomas, Technical Portfolio Lead

Bryan Morreale, Executive Director, Research & Innovation Center

This page intentionally left blank.

Table of Contents

List of Figures

List of Tables

Acronyms, Abbreviations, and Symbols

Term	Description
CEC	Cation exchange capacity
DOE	U.S. Department of Energy
ICP-OES	Inductively coupled plasma -optical emission spectrometry
ICP-MS	Inductively coupled plasma -mass spectrometry
MQ	Milli-Q water, term used to describe ultrapure water
EPK	Edgar Plastic Kaolinite
Gd	Gadolinium
La	Lanthanum
PLS	Pregnant leachate solution
PP	Polypropylene
PVC	Polyvinyl chloride
HDPE	High density polyethylene plastic
HP	Horsepower
REE	Rare Earth Elements
Sc	Scandium
SEM	Scanning electron microscopy
SEM-EDS	Scanning electron microscopy-energy dispersive spectrometry
UCC	Upper continental crust
Y	Yttrium
Yb	Ytterbium

Acknowledgments

This work was performed in support of the U.S. Department of Energy's (DOE) Fossil Energy and Carbon Management, Rare Earth Elements/Minerals Sustainability Field Work Proposal. The authors wish to thank R. Burt Thomas (NETL RIC) and Thomas Tarka (NETL RIC) for programmatic guidance, direction, and support.

ABSTRACT

Maximum rare earth element (REE) extractability from a sample of Middle Kittanning coal seam underclay was previously demonstrated at ~30% of the total REE content with a citric acid solution (Montross et al., 2020). This report further refines the mechanisms of citrate application for leaching of coal seam underclays using an organic acid lixiviant and evaluates strategies to begin to scale this process to industrially relevant volumes. This study evaluates the suitability of citrate leaching solutions for downstream recovery and separation of the REEs via oxalic acid precipitation. The applicability of citric acid solutions to recover ion-adsorbed metals from clay surfaces was evaluated by leaching a prepared sample of kaolinite with known amounts of ion-adsorbed lanthanum. Citrate systematics was further defined through experiments varying the solution pH. Up-scaling investigations proceeded with percolation leaching columns and stirred tank reactors. Two embodiments were run in percolation leaching: a continuous flow-through process and a multi-stage saturated process. The results showed that in certain limited scenarios, low pH citrate solutions could be used to target REEs mineralized within secondary calcium phosphate minerals. Results from the upscaling attempts encountered difficulties in extraction efficiencies. For the percolation columns, hydrodynamic flow was insufficient to recover the extractable REE content fully. For the stirred barrels, mixing inefficiencies likely inhibited the extractability of the REEs. Oxalic acid precipitation experiments also highlighted difficulties in downstream operations. The REEs were removed from the citrate solution with high efficiency, but were accompanied by equally efficient removal of calcium in orders of magnitude of greater amounts. Overall, for citrate leaching to be effective, future studies will have to: 1) carefully consider the feedstock application (i.e., likely better suited for secondary mineralization of calcium phosphate minerals), and 2) overcome the technical barriers of large-scale processing, such as inefficient hydrodynamic regimes due to small crush sizes needed and difficulties in downstream separation and purification. Alternatively, citrate solutions may be better recommended as leaching amendments to other leaching solutions to enhance REE complexation in the solution.

1. INTRODUCTION

Extracting rare earth elements (REEs) from easily accessible materials such as coal waste streams and coal-adjacent rock strata remains a developing option for bolstering the U.S. domestic supply of REEs and other critical metals. These materials represent waste rock from current and legacy coal mining activities or rock layers exposed after coal has been mined and removed. Underclay layers directly below a coal seam, in particular, are thought to hold the potential to host REEs remobilized during alteration processes (e.g., Schatzel and Stewart, 2003; Rozelle et al., 2016; Montross et al., 2020). Mechanistic analogs may be drawn from the ion-adsorbed clays exploited in southern China, where intense temperate weathering processes on paleosol provinces mobilize the REEs into clay-rich layers which capture the metals via ion exchange interactions (e.g., Bao and Zhao, 2008; Moldoveanu and Papangelakis, 2012). Appalachian Basin underclays, however, have exhibited only moderate enrichments of the REEs with a range from 250–750 ppm (Yang et al., 2020; Bauer et al., in prep). Nonetheless, the ease of accessibility for the underclay materials in the Appalachian Basin and the possibility of extracting critical metals as value-added products make further explorations attractive. A portion of the REE content exists as ion-exchangeable components or within secondary mineral structures, although the majority of the REE is presumed to exist as refractory primary minerals such as monazite or xenotime (Yang et al., 2020; Bauer et al., in prep). Targeting the refractory primary minerals entails an intensive beneficiation, mineral separation, and processing circuit. Targeting the easily-extractable phases of the REE, however, may present options to employ less energy intensive and more environmentally friendly methods that still represent value in critical metal extractions.

Previous work has documented moderate extractability of REEs from coal seam underclays (up to 30% of the total REE content) in the Appalachian Basin using a citric acid solution (Montross et al., 2020). Citric acid, with its three carboxylic acid functional groups, was considered an alternative lixiviant to stronger mineral acid solutions to target the ion-exchangeable and secondary mineral phases of underclays. Additionally, the distribution of REEs extracted in the citrate solutions shows a proclivity towards the more critical middle and heavy mass REEs, although this signal may be attributable to the signature of the REE host minerals. This report evaluates the scalability of these initial experimental results from test tubes on the benchtop to embodiments reflective of heap leach or vat leaching operations and stirred tank reactors.

The underclay sample selected for further upscaling investigations was an example from the Middle Kittanning coal seam and originates from a currently operating metallurgical coal mine in eastern West Virginia. The Middle Kittanning coal seam was deposited as part of the Allegheny Group during the Middle Pennsylvanian period as a northeast prograding system within a foreland basin adjacent to the Allegheny fold and thrust belt (Wright and Erber, 2018). Characterization of this underclay sample through chemical analyses, microanalytical inspection and sequential leaching documented a bulk REE concentration of ~300 ppm with relative enrichments of middle mass REE over heavy and light REE when normalized to upper continental crust (UCC) averages (Yang et al., 2020). Occurrences of secondary, phosphate-containing minerals (likely reflecting hydroxyapatite) were observed under scanning electron microscopy (SEM) and electron microprobe analysis. Sequential leaching of the Middle Kittanning underclay showed REEs associated with exchangeable and oxidizable phases within the sample (Bauer et al., in prep).

This report documents the parameters maximizing the extraction of REEs from the Middle Kittanning underclay sample using a citric acid lixiviant and reports on investigative studies for upscaling leaching operations to heap leach or stirred tank reactor embodiments. The suitability of citric acid to recover pure ion-exchangeable metals from a clay surface and the effect of pH on REE extractability were investigated. Packed column experiments mimicked conditions necessary for percolation leaching for either heap leach or vat leach type of operations. Large, stirred tank reactions were assessed using a 55-gallon barrel and impeller setup. Finally, the applicability of citrate leaching solutions for downstream processing and purification steps was assessed through oxalic acid precipitation experiments. The results presented here are to provide information on the pitfalls and considerations necessary to invoke large-scale leaching of underclay with citric acid. The Middle Kittanning underclay showcased relatively low levels of REE extraction that were exacerbated by difficult hydrodynamic conditions and/or inefficient mixing levels. Successful implementation will need to consider underclay feedstocks with higher enrichments of REEs within secondary mineral phases.

2. METHODS

2.1 FEEDSTOCK PREPARATION

Middle Kittanning underclay material (UC-12 MKT) was received as run-of-mine material taken directly from the mine wall. This material was reduced further in size using a hammer before being fed into a jaw crusher. This first crushing run produced an output of ~1/4 in. sized material. For the third column experiment and the first experiment conducted in the mixing barrels, a second crushing run was conducted in the smaller chipmunk crusher set to an opening of ~1/32 in. Sieve analyses were conducted on the sample splits for the crushed material (Figure 1).

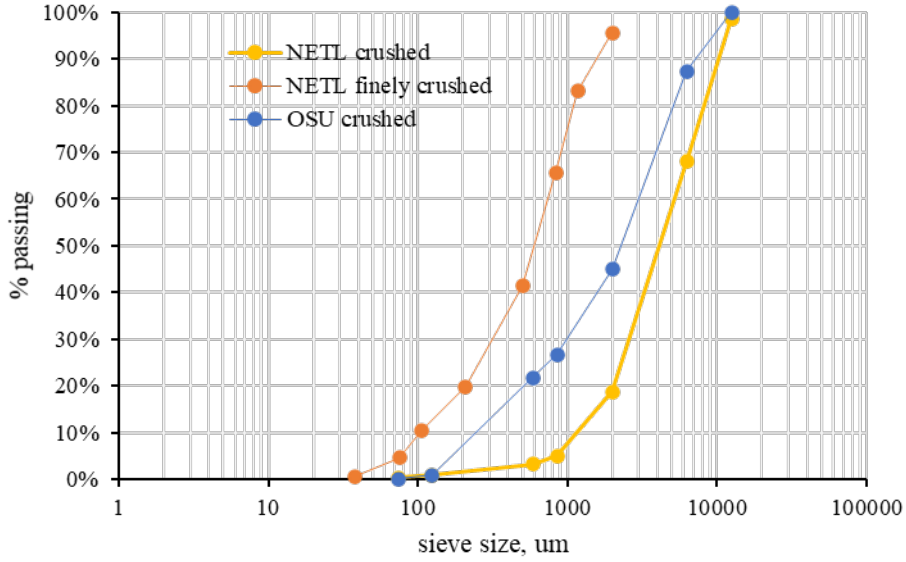

Figure 1: Particle size distribution of the prepared material.

2.2 LANTHANIDE DESORPTION FROM CLAY SURFACES

The efficacy of citrate to recover strictly outer-sphere, electrostatically-sorbed metals from clay surfaces was evaluated through an experiment where a standard clay sample was saturated with a $LaCl_3$ solution to produce a clay with known amounts of ion-adsorbed La. This La-doped clay was then reacted with citric acid, ammonium sulfate, and sodium chloride, and the resulting chemical composition was measured via inductively coupled plasma -optical emission spectrometry (ICP-OES) and -mass spectrometry (ICP-MS).

The standard clay used was a sample of Edgar Plastic Kaolinite (EPK) from Edgar Minerals (Edgar, FL). This material is well-characterized, with a specific surface area of 28.52 m^2/g, a median particle size of 1.36 µm, and a cation exchange capacity (CEC) of 4.5 meq/100 g. A 500 ppm lanthanum (La) solution at pH 5.3 was prepared from a $LaCl_3$ salt. Next, 45 mL of the 500 ppm La solution was reacted with 4.5 g of EPK in a polypropylene centrifuge tube in an end-over-end shaker for 24 hours. After 24 hours, the slurry was centrifuged, the supernatant decanted, and the solids rinsed with Milli-Q® (MQ) water and centrifuged repeatedly until

conductivity values indicated the complete removal of the $LaCl_3$ solution. The solids were then dried overnight at 50 °C. From ICP-MS analysis, this saturation process produced a kaolinite clay with 3,200 ppm La ostensibly electrostatically bound to sorption sites. Mass balances between solution and solid analyses accounted for 97% of the La mass, thus indicating good agreement and accuracy in the saturation process.

The La enriched kaolinite was split into 3 g subsamples and reacted in 30 mL of solution for 24 hours in an end-over-end rotator. These solutions included 0.1 M citric acid, 0.5 M ammonium sulfate, and 0.5 M sodium sulfate. All solutions were adjusted to pH 2 based on the native pH of 0.1 M citric acid to standardize conditions across the experiment. Following the reaction, slurries were centrifuged, the supernatant decanted, and the solids rinsed and dried as before. All solutions were filtered and acidified to pH <2 with trace metal grade HCl for subsequent analysis.

2.3 PH EXPERIMENTS

Benchtop experiments were conducted on the finely crushed material to evaluate the impact of pH on the extractability of REEs. These experiments were conducted in 50 mL polypropylene (PP) centrifuge tubes, placed in an end-over-end rotator, and reacted at ambient temperature (20-25 °C) for a total of 48 hours. Approximately 4.5 g of material was reacted with 45 mL of solution. Solution compositions are listed in Table 1. Buffered solutions made up of 0.1 M citrate were prepared from pH 2–8, inclusive of values reflecting the three pKa's of citric acid (Table 1). Mineral acids (HCl, H_2SO_4) were reacted at mildly acidic pH values. An additional set of reactions were run with higher concentration (2.4 N) mineral acid solutions and at elevated temperatures of ~80 °C for 4 hours to obtain a maximum extractability endmember. Salt solutions of ammonium sulfate $(NH_4)_2SO_4$ and sodium chloride (NaCl) were also reacted as a comparison to ion-exchange lixiviants. The concentrations of the ammonium sulfate and sodium chloride were standardized to match to the normality of the cation species (e.g., Na+) present in the 0.1 M citrate solutions.

Table 1: pH Values of Reacted Benchtop Solutions

	pH							
	<1	**2.0**	**3.1**	**4.0**	**4.8**	**5.5**	**6.0**	**8.0**
citrate buffer								
0.1 M citrate		X	X	X	X	X	X	X
mineral acids								
2.4 N HCl	X							
2.4 N H_2SO_4	X							
$6x10^{-3}$ N H_2SO_4		X						
$3.6x10^{-3}$ N H_2SO_4			X					
$9.0x10^{-7}$ N H_2SO_4				X				
salt solutions								
0.015 N $(NH_4)_2SO_4$		X				X		X
0.31 N NaCl		X				X		X
control solutions								
MQ water							X	

2.4 PERCOLATION LEACHING THROUGH PACKED COLUMN EXPERIMENTS:

Small-scale, packed column experiments were conducted to assess the applicability of citrate leaching to heap or vat leaching embodiments. Crushed material was loaded into a 3–4-in. diameter polyvinyl chloride (PVC) column to a packed depth of 20–30-in. in multiple "lifts" of ~1 kg each. This volume equated to a dry mass of 4-6 kg of underclay material used, bulk densities of 1.4–1.6 g/cm^3, and estimated macro-porosities of 30% (Table 2). Two main embodiments were tested: (1) a continuous, flow-through leach where the application rate was controlled as a function of the estimated hydraulic conductivity, and (2) a multi-stage, saturated leach (Figure 2).

Table 2: Experimental Parameters Defining the Column Experiments

	Continuous Flow-Through		Multi-Stage Saturated	
Crush size, P80	850 um < D < 8 mm	850 um < D < 8 mm	8 mm	1 mm
Dry weight, kg	3.3	3.5	6.1	3.6
Bulk density, kg/m^3	1.53	1.63	1.55	1.49
Porosity	31%	26%	29%	39%
Solution comp	0.1 M citrate	0.089 M $(NH_4)_2SO_4$	0.1 M citrate	0.1 M citrate
Final leach ratio	1.04	1.06	1.4	1.5
Total leach time	50 hrs	50 hrs	31 days	91 days

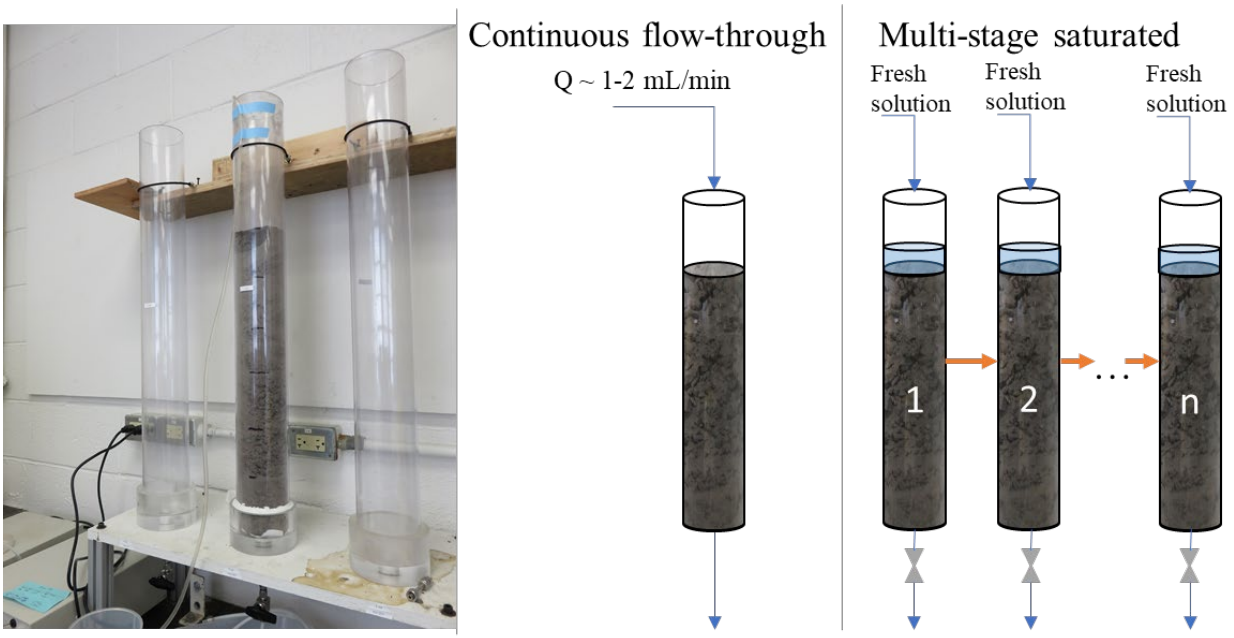

Figure 2: Column setup and operational differences for continuous flow-through and multi-stage saturated embodiments

2.4.1 Saturated Hydraulic Conductivity

Saturated hydraulic conductivity tests were initiated using an approximate constant head method. Tap water was carefully poured by hand into the top of the column to an arbitrarily defined point 3 ¾ in. from the top of the packed column. A small 50 mL beaker was placed at the outlet and allowed to fill completely; this outlet was measured at 9 in. from the bottom of the packed column, resulting in a total measured hydraulic head of 42 ¾ in. Any outflow would then overfill from this smaller beaker into the surrounding secondary containment. The level at the top of the column was maintained by hand, as the pumps could not provide a high enough flow to maintain the water level. Five-minute intervals were repeated three times, with the overflow volumes collected and measured. With the inherent uncertainties surrounding this method

application, the saturated hydraulic conductivity levels are regarded as semi-quantitative estimates only.

Stirred Tank Reactor Experiments:

Experiments were conducted in 55-gallon barrels to evaluate the scalability of citrate leaching in a stirred tank reactor. Chemical-resistant barrels constructed of high-density polyethylene (HDPE) were used for these experiments with a 0.93 horsepower (HP) pneumatic-driven impeller. The impeller was powered by compressed air supplied from a site-wide compressor delivering air at ~80 psi. Both the impeller shaft and impeller blades were constructed from 316 stainless steel. The barrels were operated with 100 L of solution to a mass of 10 kg of underclay material at ambient temperatures (15–20 °C) and ~800 rpm of agitation. Total reaction times were operated from 2 to 21 days, with periodic sampling of the liquids at specified time points.

Figure 3: 55-gallon barrel experimental setups with 4 in. axial impeller installed.

2.5 OXALIC ACID PRECIPITATION EXPERIMENTS

2.5.1 Artificial Leaching Solutions

Artificial solutions were created to mimic the compositions of citrate leaching solutions and isolate the effects of gangue element content (i.e., Fe, Ca, Al) and the presence of citrate on the precipitation efficiencies of REEs with oxalate. Gangue element concentrations were created at 4.6 mmol/L Al (BeanTown Chemical), 6.8 mmol/L Ca (Sigma-Aldrich), and 3.3 mmol/L Fe (EMD Chemicals) using chloride salts. REE solutions were created at 9.2 mmol/L with two solutions tested—one solution containing only La and a second solution containing Sc, La, Gd, Y, and Yb—using REE chloride salts (BeanTown Chemical). Citrate concentrations were

maintained at 100 mmol/L, except for solution testing the effect of citrate on gangue element precipitation, in which case there was no citrate present. All solutions were made up to an oxalic acid concentration of 100 mmol/L, and the pH maintained at approximately 1.3. All artificial leaching solutions were run in duplicates.

2.5.2 Pregnant Leachate Solutions

Multiple rounds of pregnant leachate oxalic acid precipitation experiments were conducted. The first round was conducted in 1 L Erlenmeyer flasks with ~675 mL of pregnant leachate solution (PLS) added to each Erlenmeyer flask. Post reaction recovery of the precipitate was attempted via the solution being poured over a filter paper at the top of a Buchner funnel. Minimal precipitate was recovered. Subsequent PLS-oxalic acid precipitation experiments occurred in 50 mL centrifuge tubes in duplicate in the same manner as the artificial solution experiments. Precipitate recovery was also low for these experiments, and only qualitative results from PAL analysis were received.

3. RESULTS

3.1 LANTHANIDE DESORPTION FROM KAOLINITE

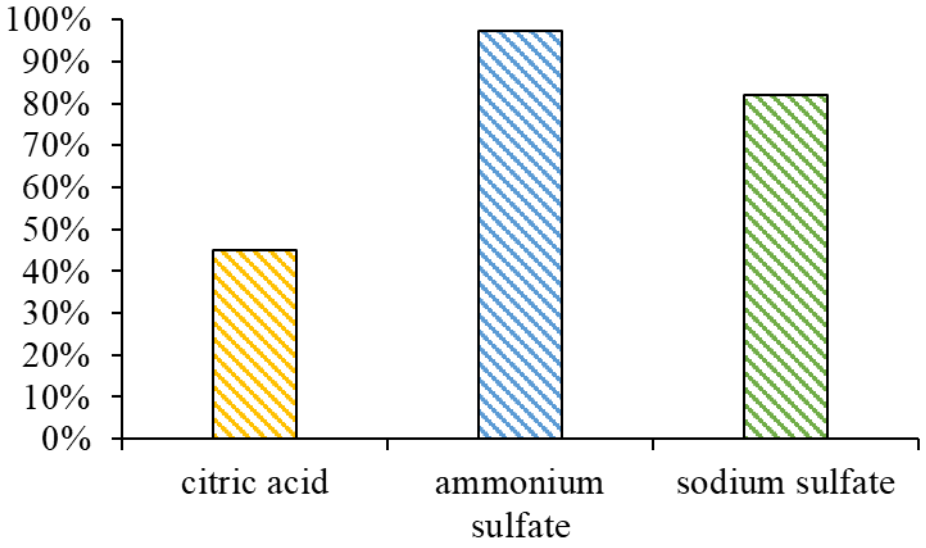

Figure 4: La recovery from La-saturated kaolinite.

Citric acid at pH 2 recovered ~45% of the sorbed La from the kaolinite surface compared to 97% and 82%, respectively, for ammonium sulfate and sodium sulfate (Figure 4). Citric acid also recovered less than 6% of the intrinsic REE content of the kaolinite. Ammonium sulfate and sodium sulfate solutions recovered ~8% of the intrinsic REE. Here, the term intrinsic REE is used to distinguish the natural composition of the kaolinite clay prior to La sorption. All solutions showcased a linear enrichment of the heavy REEs over the light REEs with positive anomalies in Eu and Y (Figure 5).

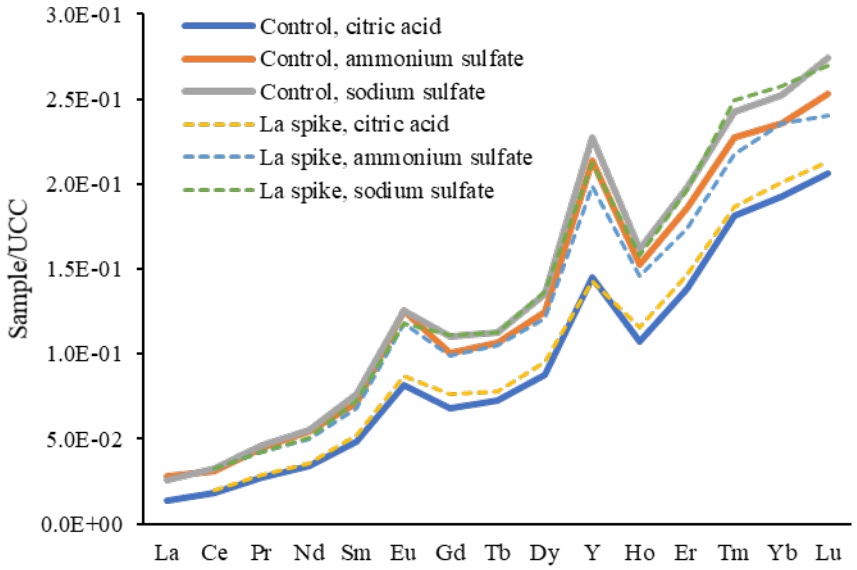

Figure 5: UCC-normalized REE distributions for all solutions. La is omitted from the plot of the "La-spike" solutions for clarity.

3.2 EFFECT OF PH ON LEACHING FROM MIDDLE KITTANNING UNDERCLAY

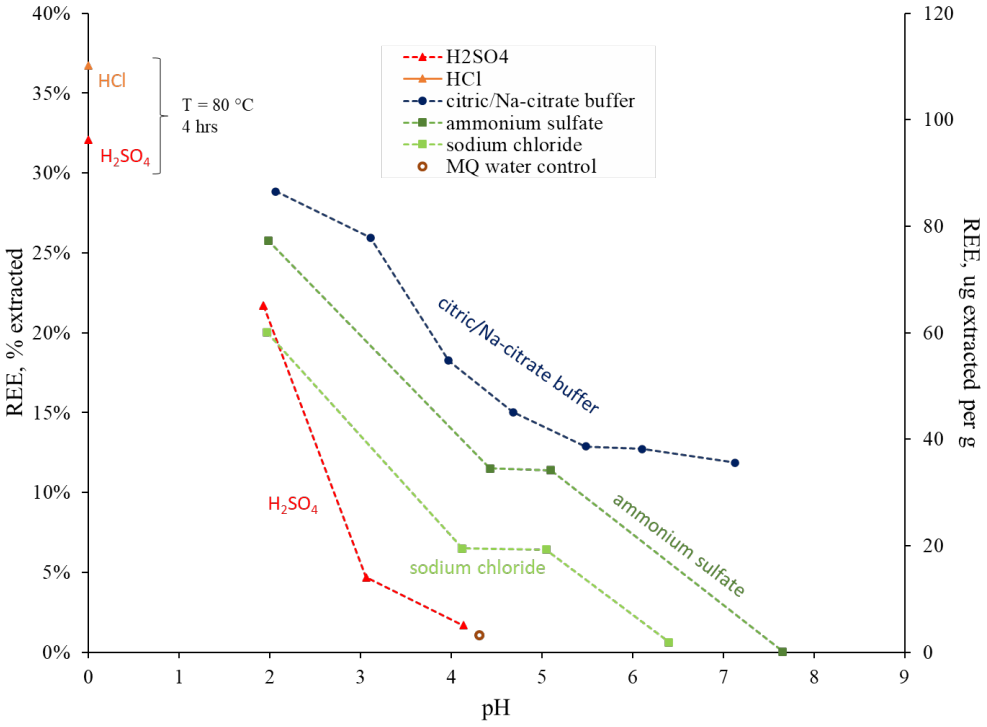

Figure 6: REE extraction as a function of pH for the tested solutions.

In general, the leaching results of the Middle Kittanning underclay show an increased extractability of total REE with lower pH (Figure 6). With the citrate solutions, up to 30% of total REE is extracted at pH ~2. This extraction with citrate solutions declines to approximately 15% of total REE with increased pH to circumneutral values. At all pH values, citrate solutions extract greater amounts of REE than ammonium sulfate or sodium chloride solutions. The more aggressive conditions utilizing 2.4 N mineral acids and elevated temperatures showed extractions of ~32–37% of total REE. In all solutions, the extracted REE showed a distinct middle REE enrichment relative to UCC values (Figure 7).

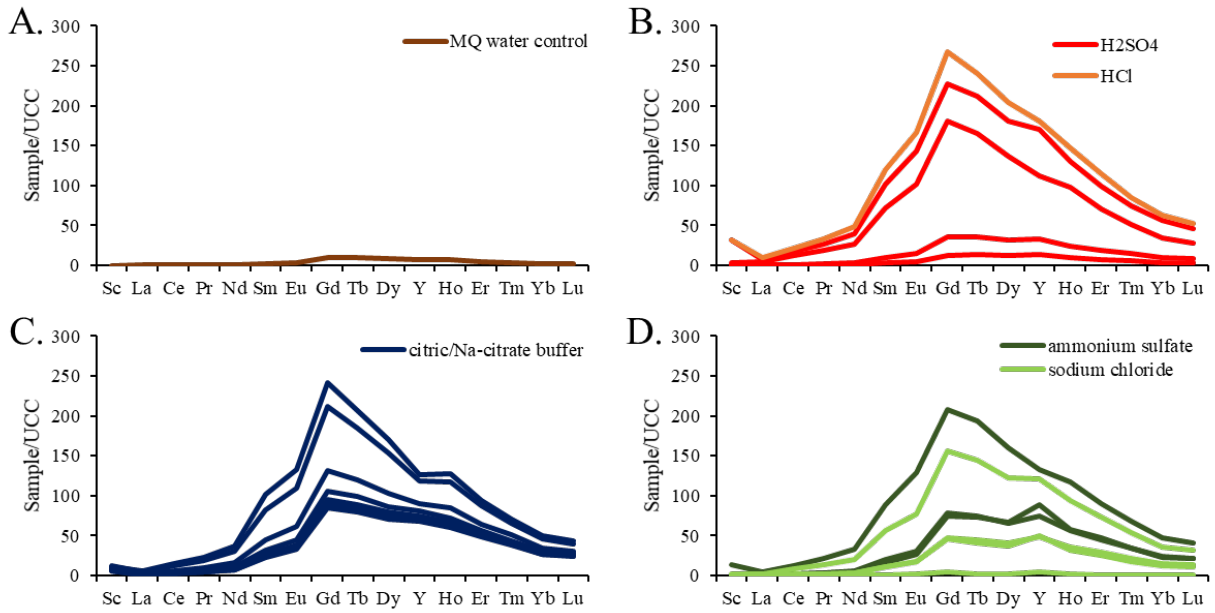

Figure 7: REE distribution patterns normalized to UCC.

3.3 PERCOLATION LEACHING THROUGH PACKED COLUMNS

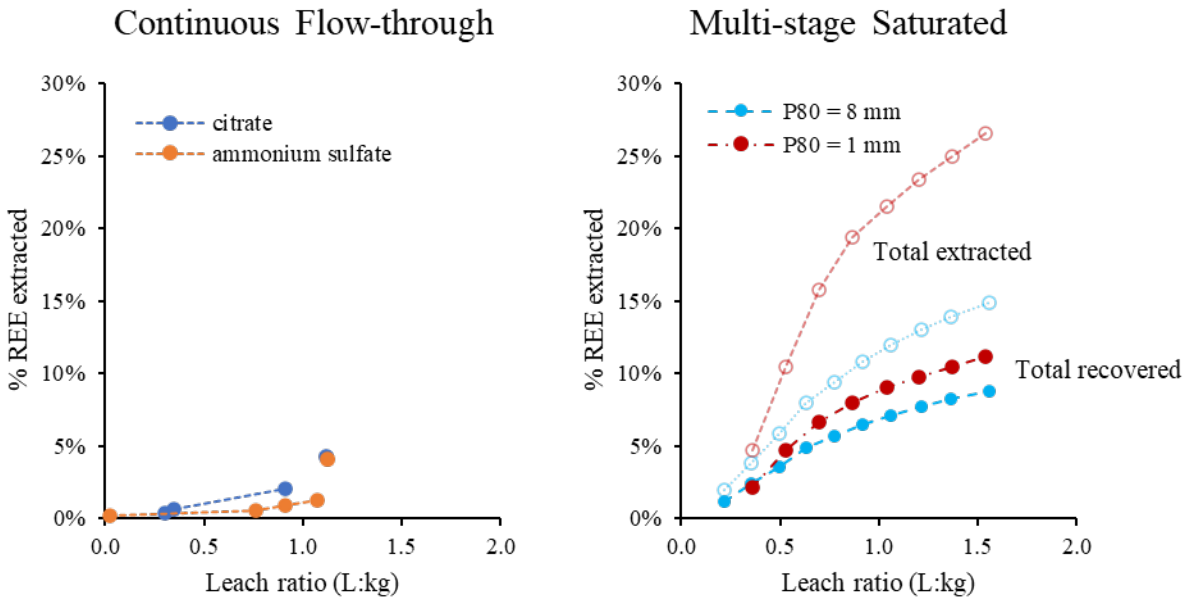

Figure 8: Leaching curves for the packed column experiments. Total extracted curves (dashed lines) for the multi-stage saturated experiments represent total solution concentrations, including solution entrained in pore spaces. Total recovered curves (solid lines) represent REE concentrations in solutions recovered off of the column.

Only a subset of timepoints was able to be analyzed for the continuous flow-through experiments due to sample loss during shipping. Nevertheless, the results showed little separation between the citrate and ammonium sulfate solutions. A maximum recoverability of ~5% of total REE was measured in solutions from the continuous flow-through column (Figure 8). By contrast, the multi-stage saturated columns showed slightly improved recoverability values of 9–10% for both the coarse (P80 = 8 mm) and fine (P80 = 1 mm) packed columns. However, the amount of solution retained on the columns after drain-down for each stage was significant, accounting for ~500–800 mL for the coarse column and ~700–900 mL for the fine column (Table 3). Collected volumes, by comparison, ranged from 800–1000 mL for the coarse column and 600–750 mL for the fine column. Taking into account these retained volumes of solution in the columns, the total extracted REE curves approached ~15% and 30% for the coarse and fine columns, respectively (Figure 8). Only a fraction of the solution was able to be recovered through draining the column under gravity alone, in which 9–10% total REE was actually recovered.

Table 3: Multi-Stage, Saturated Column Volumes Loaded, Collected, and Retained

P80 = 8 mm		Volumes, mL			P80 = 1 mm		Volumes, mL		
Sample	Leach Ratio	Loaded	Collected	Retained	Sample	Leach Ratio	Loaded	Collected	Retained
PV1	0.2	1334	819	516	PV1	0.4	1300	593	707
PV2	0.4	830	828	518	PV2	0.5	600	590	717
PV3	0.5	851	821	548	PV3	0.7	620	468	869
PV4	0.6	844	838	554	PV4	0.9	608	575	902
PV5	0.8	866	820	600	PV5	1	614	736	780
PV6	0.9	854	839	616	PV6	1.2	599	534	845
PV7	1.1	859	823	652	PV7	1.4	598	623	821
PV8	1.2	938	915	676	PV8	1.5	614	619	600
PV9	1.4	927	917	686					
PV10	1.6	1195	1055	826					

3.4 STIRRED REACTIONS IN 55-GALLON BARRELS

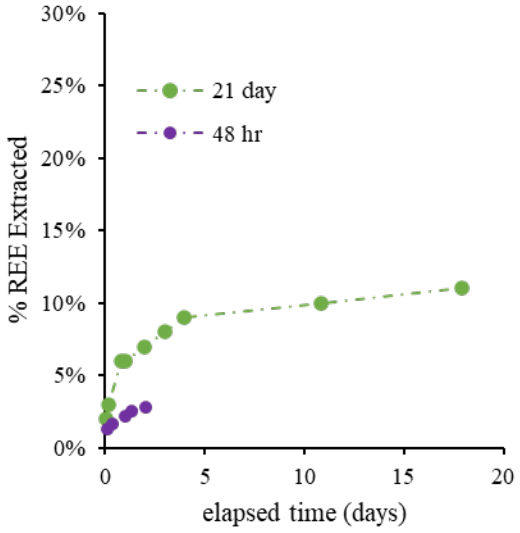

Figure 9: 55-gallon barrel REE extraction curves.

A maximum of ~10% REE extraction was achieved after continuous mixing with the axial flow impeller after 5 days of continuous operation (Figure 9). After 5 days, only marginal gains in total REE extraction were observed continuing out to 21 days of operation. Despite utilizing a finer particle size distribution, the initial experiments conducted with a flat-bladed mixing impeller only achieved a total REE extraction of ~6% after 48 hours, and the extraction curve can clearly be seen with a flattened slope relative to the extraction curve with the axial flow impeller.

3.5 OXALIC ACID PRECIPITATION

The presence of citrate in solution in equimolar amounts to oxalic acid showed no discernable impact on the removal efficiencies for the gangue elements in the artificial solutions (Table 4). Calcium was removed to a highly efficient extent (up to 94% removal from solution), 2–7% of the total aluminum removed from solution, and effectively none of the iron precipitated out, regardless of the citrate content.

Table 4: Effect of Citrate Presence for Removal Efficiencies of Gangue Elements in Artificial Solutions

% Removal From Solution		
	no citrate	citrate
Fe	0	0
Al	2	7
Ca	94	94

Oxalic acid precipitation proved highly efficient in precipitating the REEs from solution, regardless of the presence of gangue elements. The removal of REEs from solution was practically quantitative for the representative elements chosen (99–100%), except for scandium, which had lower removal efficiencies of 73%. Notably, very little Fe and Al precipitated from solution (0–7%). Calcium, however, showed similar removal efficiencies to the REEs, averaging 88–92% removal (Table 5).

Table 5: Effect of Gangue Elements on Removal Efficiencies of the REE in Artificial Solutions

% Removal From Solution		
	no gangue	gangue
La	100	100
5 REE	-	94
Fe	-	0
Al	-	7
Ca	-	92

Similar efficiencies were observed for oxalic precipitation in experimental citrate leaching solutions. Nearly all of the REEs were removed from solution, with very little Fe and Al coming out of solution. Calcium, however, displayed slightly lower removal efficiencies in these experimental solutions of ~69%.

4. DISCUSSION

4.1 EFFECTIVENESS OF CITRATE FOR ION-ADSORBED AND/OR SECONDARY MINERAL METALS

From the desorption experiments on La-doped kaolinite surfaces, citric acid at pH 2 is clearly least effective relative to ammonium sulfate and sodium sulfate in recovering a purely electrostatically bound, outer-sphere metal species from clay surfaces. The role of the pH of the solution undoubtedly affects the extraction yields. At pH 2, citric acid exists as H_3-citrate, with little driving force for ligand-promoted complexation. At progressively higher pH values, the carboxylic acid groups subsequently deprotonate, rendering H_2-citrate$^-$, H-citrate^{2-}, and citrate^{3-} species that are more available for ligand complexation with metal species. The nature of REE complexation with the citrate anion is complex and not fully resolved in the literature, but the simplest case is as a 1:1 complex of Ln^{3+} with citrate^{3-}, where Ln represents the lanthanide elements (e.g., Xiong, 2011; Zabiszak et al., 2018; Janusz et al., 2020). Thus, the preference for ligand-complexation can be seen to be favored at high pH values. However, operating at higher pH values would have necessitated the addition of either NaOH or trisodium citrate to the solution, both of which would have introduced Na^+ counterions to the system and, by extension, an ion-exchange capacity. With these caveats in mind and for the specified conditions, citric acid is not as effective as ammonium sulfate or sodium sulfate in removing purely ion-exchangeable species on clay surfaces.

For the Middle Kittanning underclays, however, the REE content is not hosted exclusively as ion-exchangeable species on the clay surfaces. At least 30% of the total REE content is expected to reside within secondary mineral occurrences, based on scanning electron microscope-energy dispersive spectrometry (SEM-EDS) inspection and sequential digest results (Yang et al., 2020; Bauer et al., *in prep*). In cases where the REE exist in phases other than ion-exchangeable species on clay surfaces, citrate-based lixiviants show a clear advantage in extractability over simple ion-exchangeable salt solutions (Figure 5). All solutions show increased yields with lower pH values, indicating the existence of a proton-promoted dissolution mechanism. The additional advantage of citrate solutions in these cases is likely attributable to the added effect of a ligand-promoted dissolution mechanism. For secondary minerals such as apatite, organic acids have been demonstrated to effectively enhance dissolution rates through interactions of the organic ligand both at the mineral surface and in solution (e.g., Misra, 1996; Misra, 1999; Goyne et al., 2010). At the mineral surface, organic ligands can complex to the metal species (e.g., Ca, Fe, REEs), essentially weakening the bonds within the mineral lattice and effectuating dissolution (Misra, 2016; Misra, 1999). Released metal cations can also be complexed by the organic ligand in solution, effectively removing a product of the dissolution reaction and promoting additional reactivity according to Le Chatelier's principle (Wyrzykowskiw and Chmurzynski, 2010; Vavrusova and Skibsted, 2016). Additional corroborating evidence for the existence of secondary mineral phases for the REEs is observed through correlations between REEs and other cationic species, namely Ca, P, Fe, and Al, and is discussed in the following section.

4.2 CORRELATION OF REES WITH MAJOR CATIONS

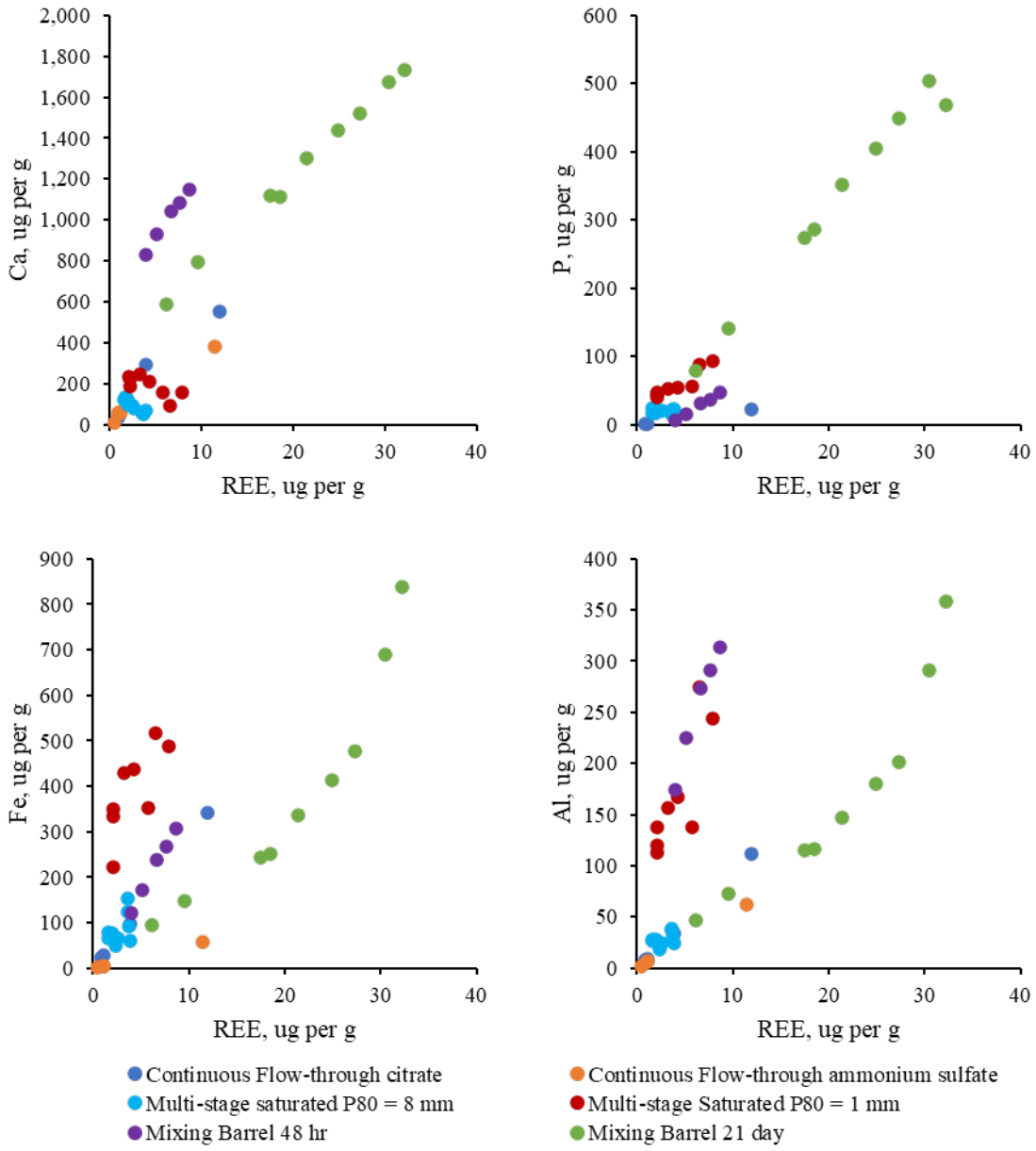

Figure 10: Crossplots between extracted REEs and Ca, P, Fe, and Al.

In the leaching solutions from the column (both continuous flow-through and multi-stage saturated embodiments) and the mixing barrel experiments, the extracted REEs showed positive correlations to extracted Ca, Fe, P, and Al (Figure 10). In all cases, the extracted REE mass was 2–3 orders of magnitude lower than the mass of these base metals, foreshadowing the difficulties in separating the REEs into saleable products in downstream operations (see oxalic acid precipitation section). The correlation of extracted REEs with these base metals suggests: 1) the concomitant dissolution of the gangue mineralogy (e.g., aluminosilicate minerals) along with the

REE phases, and/or 2) the association of REE with Ca, Al, P (and Fe) phases. For the Middle Kittanning underclay material, the latter supposition is likely dominant, although the concomitant dissolution of gangue mineralogies is also very likely occurring. During sequential leaching experiments, the Middle Kittanning material showed a correlation of REE to a Ca, Al, P phase, likely associated with either secondary minerals such as crandallite or a form of secondary apatite (Bauer et al., in prep). Additionally, the middle REE enriched distribution patterns (Figure 7) are consistent with a secondary mineral source of REE, as these distribution patterns are similar for reworked Fe/Mn-oxides and secondary apatite phases (e.g., carbonate fluorapatite) (e.g., Yang et al., 2017; Chen et al., 2015; Cruse et al., 2000). The genesis of middle REE enriched patterns in these secondary mineral phases likely originates through competitive balances on the scavenging of lighter mass REEs to particle surfaces versus stronger complexations of the heavier mass REEs to organic matter (e.g., Ohta and Kawabe, 2000; Ohta and Kawabe, 2001), leaving a middle REE enriched distribution in diagenetic fluids to be quantitatively captured in secondary phases. The middle REE enrichments of the Middle Kittanning leachates and the correlations between REE, Ca, Al, P, and Fe suggest the dissolution of a secondary mineral host of the REE. Ligand-promoted dissolution of this secondary mineral phase likely accounts for the competitive advantage of citrate over ion-exchange lixiviants.

4.3 SCALABILITY OF CITRATE LEACHING PROCESS

The embodiments of the packed columns and the mixing barrel reactions failed to achieve the levels of REE extraction observed from bench-scale experiments. While the total extracted levels achieved in the columns were ~15% and ~30%, respectively, for the coarse and fine crushed material, the amount actually recovered from the column was ~9–10% of the total REE content. The differences between the amount of REE extracted versus the amount of REE recovered are a function of the hydrodynamics of the packed columns and the amount of solution that remains entrained within the packed material. While close to the maximum amount of REE extraction was obtained in the fine crushed column, only a small proportion of the leaching solution flowed out of the column for collection. Future considerations would need to assess options for enhanced recovery, such as the viability of a flushing solution to chase the remnant leaching solution from the column.

Mixing inefficiencies in the 55-gallon barrels were also apparent, even with extended reaction times out to 21 days. A maximum REE extraction of ~10% was seen for the mixing barrel experiments, despite solution composition (e.g., pH) and solution to rock ratios remaining relatively constant to benchtop reactions. The benchtop reactions, however, were able to be conducted in centrifuge tubes with end-over-end rotation, ensuring constant agitation and mixing. The mixing barrels were limited to a single impeller placed in a flat-bottom 55-gallon barrel with a max output of 0.93 HP. Future considerations for scaling up in mixing barrels may need to utilize more energetic mixing options or consider different reactor geometries to enhance mixing and contact.

4.4 OXALIC ACID PRECIPITATION

Multiple rounds of oxalic acid precipitation experiments indicate that Fe and Al are of low concern for co-precipitation with REE as both elements are mainly held in solution with less than 10% removed from artificial solutions and less than 1% removed from PLS. However, Ca is of higher concern as up to 92% was removed from artificial solutions, and 69% of Ca was removed

from PLS. Therefore, Ca is the gangue element of concern for co-precipitation with REE as there was a significant "contaminating" presence of Ca in the precipitate product. For all artificial solutions containing La, more than 99% of La was removed from solution. Other REE showed similar removal efficiencies except for Sc, which showed efficiencies of only ~73%. The PLS showed similar REE removal efficiencies with above 96% (including Sc) precipitated from solution. There is little effect of competing ions on La and REE precipitation as there was no difference in La removal efficiencies with the presence of gangue elements. The presence of citrate had little to no effect on the precipitation of gangue elements and REE from solution. The high removal efficiencies of the REE (excluding Sc) with the high presence of Ca will complicate downstream purification and separation abilities.

5. CONCLUSIONS

The maximum extractability demonstrated on a sample of Middle Kittanning underclay was ~30% using citric acid solutions. Citric acid was hypothesized to access both ion-exchangeable REEs as well as REEs encapsulated within relatively easily-soluble secondary mineral phases. Experimental tests conducted at low pH values, however, showed that citric acid was less effective at recovering a purely ion-exchangeable, electrostatically bound metal from a kaolinite sample than traditional ion-exchange lixiviants (i.e., ammonium sulfate, sodium sulfate). Higher pH values (not tested in this report) may conceivably increase the efficiency of ion-exchangeable REE recovery with citric acid by shifting the speciation of the citrate anion towards deprotonated species, aiding in the complexation to metal cations. However, the conditions of leaching need to be weighed against the composition of the targeted feedstock. For the Middle Kittanning underclay sample, higher pH values were less efficient at recovering the REEs than lower pH solutions and citrate solutions shown to be more effective than ion-exchangeable lixiviants. The performance of low pH citrate solutions was hypothesized to be due to the ability of citrate to effectively scavenge relatively easily-soluble secondary mineral phases, such as the hydroxyapatite phase, that are known to capture REEs in a middle REE enriched pattern.

Attempts to systematically scale this citrate leaching procedure to larger volumes and masses could not reproduce the maximum level of extractability observed in the benchtop scale experiments. For the percolation columns, inefficiencies in the fluid flow through the column were the main impediments. Flow-through embodiments failed to approach more than a fraction of the total extractability potential after a leach ratio of 1.5 solution mass to underclay mass. Multi-stage saturated attempts showed better total extractability, but the amount of fluid recovered from the column was incomplete due to the small crush sizes deemed necessary for extraction. The stirred tank reactor experiments also suffered from inefficiencies in scaling up system sizes, highlighted by difficulties in agitating a slurry solution to ensure adequate contact.

For future considerations, the technical impediments that remain to be overcome for citrate leaching of underclays include the proper design of percolation embodiments to optimize hydrodynamic performance against reactivity, as well as the proper design of agitating vessels to enact large-scale mixing experiments. Downstream applications of the citrate leaching process also would need to be refined. While oxalic acid precipitation shows an efficient scavenging of dissolved REEs in citrate solutions, these results are complicated by an equally efficient scavenging of calcium, leading to complications in separation and purification efforts. The future applications of citric acid solutions will likely need to be targeted more narrowly to feedstocks with abundant secondary mineralization (such as hydroxyapatite) and have more effective means to strip the extracted metals from the citrate solutions. Citrate could also be used as an amendment to other leaching systems in cases where enhanced complexation of secondary mineralized REEs may be warranted.

6. REFERENCES

Bao, Z.; Zhao, Z. Geochemistry of mineralization with exchangeable REY in the weathering crusts of granitic rocks in South China. *Ore Geology Reviews* **2008,** *33*, 519–535. https://doi.org/10.1016/J.OREGEOREV.2007.03.005

Bauer, S.; Yang, J.; Stuckman, M.; Verba, C. *REE and critical mineral fractions of Central Appalachian coal related strata determined by 7-step sequential extraction*; NETL Technical Report Series; U.S. Department of Energy, National Energy Technology Laboratory: Albany, OR, in preparation.

Chen, J.; Algeo, T. J.; Zhao, L.; Cao, L.; Zhang, L.; Li, Y. Diagenetic uptake of rare earth elements by bioapatite, with an example from Lower Triassic conodonts of South China. *Earth-Science Reviews* **2015,** *149*, 181–202. https://doi.org/10.1016/j.earscirev.2015.01.013

Cruse, A. M.; Lyons, T. W.; Kidder, D. L. Rare-earth element behaviour in phosphate and organic-rich host shales. *SEPM Special Publication No. 66* **2000,** 445–453.

Goyne, K. W.; Brantley, S. L.; Chorover, J. Rare earth element release from phosphate minerals in the presence of organic acids. *Chemical Geology* **2010,** *278*, 1–14. https://doi.org/10.1016/j.chemgeo.2010.03.011

Janusz, W.; Pikus, S.; Skwarek, E.; Olszewska, E. Synthesis of citrates of selected lanthanides (Er, Ho and Lu). *Physicochemical Problems of Mineral Processing* **2020,** *56*, 225–234. https://doi.org/10.37190/PPMP/128739

Misra, D. N. Interaction of citric acid with hydroxyapatite: Surface exchange of ions and precipitation of calcium citrate. *Journal of Dental Research* **1996,** *75*, 1418–1425. https://doi.org/10.1177/00220345960750061401

Misra, D. N. Interaction of Citric or Hydrochloric Acid with Calcium Fluorapatite: Precipitation of Calcium Fluoride. *Journal of Colloid and Interface Science* **1999,** *220*, 387–391. https://doi.org/10.1006/JCIS.1999.6537

Moldoveanu, G. A.; Papangelakis, V. G. Recovery of rare earth elements adsorbed on clay minerals: I. Desorption mechanism. *Hydrometallurgy* **2012,** *117–118*, 71–78. https://doi.org/10.1016/j.hydromet.2012.02.007

Montross, S. N.; Yang, J.; Britton, J.; McKoy, M.; Verba, C. Leaching of Rare Earth Elements from Central Appalachian Coal Seam Underclays. *Minerals* **2020,** *10*, 577. https://doi.org/10.3390/MIN10060577

Ohta, A.; Kawabe, I. (2000). Rare earth element partitioning between Fe oxyhydroxide precipitates and aqueous NaCl solutions doped with NaHCO3: Determinations of rare earth element complexation constants with carbonate ions. *Geochemical Journal* **2000,** *34*, 439–454. https://doi.org/10.2343/geochemj.34.439

Ohta, A.; Kawabe, I. REE(III) adsorption onto Mn dioxide (δ-MnO2) and Fe oxyhydroxide: Ce(III) oxidation by δ-MnO2. *Geochimica et Cosmochimica Acta* **2001,** *65*, 695–703. https://doi.org/10.1016/S0016-7037(00)00578-0

Rozelle, P. L.; Khadilkar, A. B.; Pulati, N.; Soundarrajan, N.; Klima, M. S.; Mosser, M. M.; Miller, C. E.; Pisupati, S. V. A Study on Removal of Rare Earth Elements from U.S. Coal

Byproducts by Ion Exchange. *Metallurgical and Materials Transactions E* **2016,** *3*, 6–17. https://doi.org/10.1007/s40553-015-0064-7

Schatzel, S. J.; Stewart, B. W. A provenance study of mineral matter in coal from Appalachian Basin coal mining regions and implications regarding the respirable health of underground coal workers: A geochemical and Nd isotope investigation. *International Journal of Coal Geology* **2012,** *94*, 123–136. https://doi.org/10.1016/j.coal.2012.01.011

Vavrusova, M.; Skibsted, L. H. Aqueous solubility of calcium citrate and interconversion between the tetrahydrate and the hexahydrate as a balance between endothermic dissolution and exothermic complex formation. *International Dairy Journal* **2016,** *57*, 20–28. https://doi.org/10.1016/j.idairyj.2016.02.033

Wright, C. E.; Erber, N. R. *Evaluation of available resources of the Middle Kittanning (No. 6) and Lower Kittanning (No. 5) coal beds in Ohio;* Columbus, Ohio Department of Natural Resources; Division of Geological Survey Open-File Report 2018-1, 2018; p. 24.

Wyrzykowski, D.; Chmurzyński, L. Thermodynamics of citrate complexation with Mn2+, Co 2+, Ni2+ and Zn2+ ions. *Journal of Thermal Analysis and Calorimetry* **2010,** *102*, 61–64. https://doi.org/10.1007/s10973-009-0523-4

Xiong, Y. Organic species of lanthanum in natural environments: Implications to mobility of rare earth elements in low temperature environments. *Applied Geochemistry* **2011,** *26*, 1130–1137. https://doi.org/10.1016/j.apgeochem.2011.04.003

Yang, J.; Montross, S.; Britton, J.; Stuckman, M.; Lopano, C.; Verba, C. Microanalytical Approaches to Characterizing REE in Appalachian Basin Underclays. *Minerals* **2020,** *10*, 546. https://doi.org/10.3390/min10060546

Yang, J.; Torres, M.; Mcmanus, J.; Algeo, T. J.; Hakala, J. A.; Verba, C. (2017). Controls on rare earth element distributions in ancient organic-rich sedimentary sequences: Role of post-depositional diagenesis of phosphorus phases. *Chemical Geology* **2017,** *466*. https://www.sciencedirect.com/science/article/pii/S0009254117304011

Zabiszak, M.; Nowak, M.; Taras-Goslinska, K.; Kaczmarek, M. T.; Hnatejko, Z.; Jastrzab, R. Carboxyl groups of citric acid in the process of complex formation with bivalent and trivalent metal ions in biological systems. *Journal of Inorganic Biochemistry* **2018,** *182*, 37–47. https://doi.org/10.1016/j.jinorgbio.2018.01.017

Brian Anderson
Director
National Energy Technology Laboratory
U.S. Department of Energy

Jessica Mullen
Federal Technology Manager Rare-Earth Elements & Critical Minerals
National Energy Technology Laboratory
U.S. Department of Energy

Anna Wendt
Program Manager
Minerals Sustainability
U.S. Department of Energy

Bryan Morreale
Associate Laboratory Director for Research & Innovation
Research & Innovation Center
National Energy Technology Laboratory
U.S. Department of Energy

R. Burt Thomas
Technical Portfolio Leader
Critical Minerals
National Energy Technology Laboratory
U.S. Department of Energy